Top Catal (2014) 57:135–142
DOI 10.1007/s11244-013-0169-0

ORIGINALPAPER

Activity and Selectivity Trends in Synthesis Gas Conversion to Higher Alcohols

Andrew J. Medford · Adam C. Lausche · Frank Abild-Pedersen · Burcin Temel · Niels C. Schjødt · Jens K. Nørskov · Felix Studt

Published online: 17 October 2013

Abstract Production of higher alcohols directly from synthesis gas is an attractive chemical process due to the high value of alcohols as fuel blends and the numerous possibilities for production of synthesis gas. Despite years of research the industrial viability of such a process is severely limited due to lack of suitable catalysts. In this work we contribute to an understanding why it has been difficult to find transition-metal higher alcohol catalysts, and point to possible strategies for discovering new active and selective catalysts. Our analysis is based on extensive density functional theory calculations to determine the energetics of ethanol formation on a series of metal (211) surfaces. The energetic information is used to construct a mean-field micro-kinetic model for the formation of ethanol via CH_x–CO coupling. The kinetic model is used along with a descriptor-based analysis to gain insight into the fundamental factors determining activity and selectivity on transition-metal surfaces.

Electronic supplementary material The online version of this article (doi:10.1007/s11244-013-0169-0) contains supplementary material, which is available to authorized users.

A. J. Medford · J. K. Nørskov
Department of Chemical Engineering, Stanford University, Stanford, CA 94305, USA

A. J. Medford · A. C. Lausche · F. Abild-Pedersen · J. K. Nørskov · F. Studt (✉)
SUNCAT Center for Interface Science and Catalysis, SLAC National Accelerator Laboratory, 2575 Sand Hill Road, Menlo Park, CA 94025, USA
e-mail: studt@slac.stanford.edu

B. Temel · N. C. Schjødt
Haldor Topsøe A/S, Nymøllevej 55, 2800 Kongens Lyngby, Denmark

Keywords Synthesis gas conversion · Higher alcohols · Density functional theory · Micro-kinetic modeling

1 Introduction

The conversion of synthesis gas to higher alcohols is a field that has attracted considerable interest due to the favorable properties of higher alcohols as fuel blends and the possibility of synthesis gas generation from a variety of carbon sources including coal gasification, natural gas and second-generation biomass [1]. Finding selective catalysts for this reaction is quite challenging, however, as many different products, e.g. methane, hydrocarbons, methanol, can be obtained in the conversion process. It is therefore of central importance to understand the underlying factors that determine selectivity in synthetic gas conversion processes if one wants to design catalysts that are highly selective to one specific product.

There are several classes of catalysts that show selectivity towards the production of higher alcohols [2–4]. Among the catalysts with the highest selectivity towards oxygenates are modified Cu-based methanol catalysts [5–7], variations of Fischer–Tropsch catalysts based on mixtures of Co, Rh, and/or Fe [8–12], and promoted molybdenum carbide [13–15] and sulfide catalysts [1, 3, 13, 14]. Yet, even for the best catalysts significant improvements in selectivity and activity need to be achieved to make synthesis gas conversion to higher alcohols attractive from a commercial point of view. So far, there have only been few theoretical studies on the mechanism of ethanol formation [16, 17] and a screening study on ethanol decomposition over various transition-metals [18]. Herein we investigate in detail one potential reaction path leading to higher

alcohol formation that is based on the insertion of adsorbed CO into CH_x species. We focus on transition metals and use scaling relations to simplify this reaction significantly. We develop a mean field microkinetic model in combination with scaling relations to enables us to single out some important properties a catalyst needs to have in order to be selective.

The fact that most higher alcohol catalysts are based on Cu or Rh, and that these metals require significant modification (via promotion with alkali, oxides, or other metals) is interesting [3]. Why is it that these two metals that are so different in nature are so similar for higher alcohol synthesis, and why are there no pure metallic catalysts that are able to produce higher alcohols selectively? We will try to shed light on why there are no pure metallic higher alcohol catalysts based on concepts for higher alcohol formation from one possible reaction path where oxygenates are formed via CH_x–CO bond coupling. We include methane and methanol formation, as these are potential products that could significantly decrease higher alcohol selectivity. The production of Fischer–Tropsch products, C3+ alcohols, and other oxygenates are excluded for simplicity and will be subject to further studies. Using the results of this model we show the reasons for the fundamental difficulty of finding catalytically active metal surfaces for higher alcohol synthesis.

2 Methods

2.1 Density Functional Theory Calculations

Adsorption energies were obtained using the plane-wave ultrasoft pseudopotential density functional theory (DFT) code DACAPO [19] with the exchange–correlation effects treated using the RPBE functional [20]. When possible, adsorption and transition-state energies were taken from previously published work [21–24] as obtained by CatApp [25]. Intermediates containing the CCO backbone were calculated using a slab model with 3 layers where the uppermost layer was allowed to relax. The (211) surface was modeled using a super-cell of size 3×1. A Monkhorst–Pack k-point grid of density $4 \times 4 \times 1$ was used to sample the Brillouin zones [26], and an energy (density) cutoff of 340 (500) eV was used. Hydrogenation barriers for intermediates with the CCO backbone are estimated from transition-state scaling for similar species [24]. A complete list of energies and their origin can be found in Table S1.

2.2 Microkinetic Modeling

The micro-kinetic model is constructed in the mean-field approximation. Rates are determined by numerically solving the coupled differential equations with the steady state approximation. In this work we have focused on the stepped (211) facets, which have been shown to be the active site for CO dissociation [27]. Four different adsorption sites were included in order to capture the complexity of this reaction on the stepped surface. The adsorption sites have been normalized to have a coverage of 1 for each site. The reader is referred to Ref. [21] for further discussion of this four-site model where it has been applied successfully for the methanation reaction [21]. Details concerning the distribution of intermediates between site types are provided in the supplementary information. Selectivity is defined as the rate of formation of the product of interest divided by the rates of formation for methane, methanol, and ethanol without any weighting for the number of carbons. Further details and all numerical inputs to the kinetic model can be found in Sect. S1 of the supplementary information.

3 Results

We base our modeling of synthesis gas conversion to oxygenates on ethanol, the simplest higher alcohol. There are several mechanisms towards oxygenates discussed in the literature [6, 16, 28–30]. Herein we focus on ethanol formation via coupling of CH_x ($x = 0 - 3$) species and adsorbed CO, which is the mechanism commonly discussed in connection with higher alcohol synthesis [6, 16]. The formed CH_xCO intermediates are in turn hydrogenated to ethanol. Formation of the CH_xCO intermediates is possible via the four following coupling steps:

(1) $C^* + CO^* \rightarrow CCO^* + *$
(2) $CH^* + CO^* \rightarrow CHCO^* + *$
(3) $CH_2^* + CO^* \rightarrow CH_2CO^* + *$
(4) $CH_3^* + CO^* \rightarrow CH_3CO^* + *$

CH_x species are formed via splitting of CO and hydrogenation of the resulting carbon as described for the methanation reaction [21, 31]. Direct insertion of CO into methanol has been suggested as a carbon–carbon coupling route [6], but is not considered in the present paper. However, C–O bond breaking of methoxy and other CH_xO intermediates (where $x = 1$–3) is included in order to allow for methanol as a source for carbonaceous species on the surface. In this way our model includes the formation of higher alcohols from a reaction mixture of synthesis gas and methanol, which is a realistic depiction of syngas chemistry on Cu catalysts.

In the present model, which we suggest to represent the most likely reaction pathway, and as we will show, it explains a number of experimental observations on trends in activity including the effect of the presence of methanol

in the reaction gas mixture. Additional pathways may contribute for certain catalysts and reaction conditions, both for the formation and consumption of ethanol, and the present model provides hence a first estimate of the ethanol production rate.

Since selectivity is a key issue, inclusion of methanol and methane as alternative products is crucial when modeling ethanol formation. Both CO hydrogenation to methane [21, 27, 31] as well as methanol [22, 32] have been described in earlier theoretical and experimental studies. Importantly, it was found that both reactions proceed much faster on step sites of transition metal surfaces as compared to close-packed terraces [27, 32]. The reaction mechanism towards the formation of higher alcohols considered here is comprised of CH_x–CO bond formation as described above. Since the transition states of bond coupling reactions are considerably stabilized on the stepped surface as compared to the close-packed surface [23, 33], we assume the stepped (211) surfaces as the active sites for ethanol formation. We will discuss the likelihood and implications of ethanol formation on less open surfaces later on.

Earlier work established trends in adsorption and transition state energies when going from one surface to the next; these trends have been used successfully to model methane as well as methanol formation, where both reactions could be fully described by only two parameters, the carbon and oxygen binding energies [21, 22, 31]. We applied these scaling relations for adsorbates [34, 35] and transition-states [23, 24, 36–38] of CH_xCO species in order to describe the reaction network described here with the same two parameters (scaling of adsorbates and transition states is shown in Sect. S3).

We can obtain the catalytic selectivity by combining the above-described analysis of ethanol formation with previous models of methane [21] and methanol synthesis. In addition methanol is considered as a second carbon source for higher alcohol formation via splitting of CH_xO species. Figure 1 shows the solution to the full microkinetic model under steady state conditions where the turnover frequency is plotted as a function of the two descriptors (the carbon and oxygen binding energy) for methane (a), methanol (b), and ethanol (c) production. By solving the combined models simultaneously the rate towards the different products can be obtained from which the selectivity towards ethanol can be derived. This is plotted in Fig. 1d.

As can be seen in Fig. 1, the methane volcano has two distinct maxima, one close to metals like Ru, Rh, and Ni and one at about 2 eV lower carbon binding energies. The

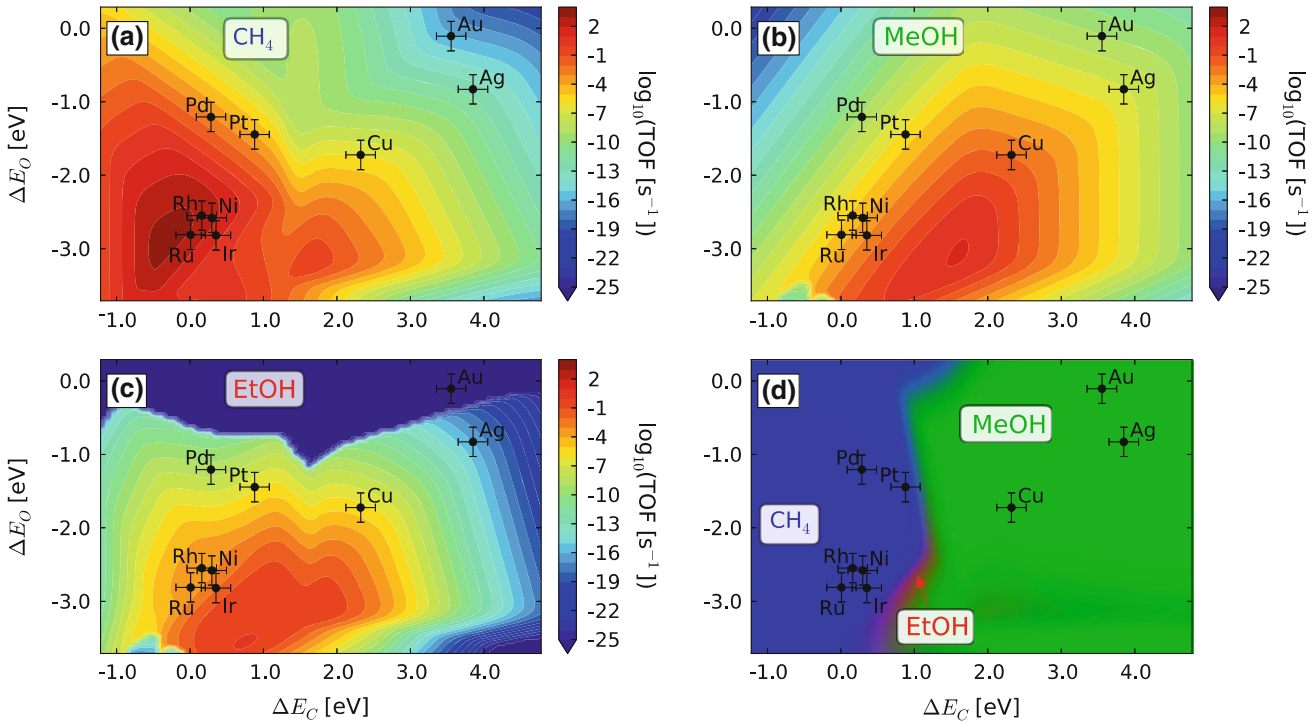

Fig. 1 **a** Calculated turnover frequencies (TOF) as a function of carbon and oxygen binding energies for methane, **b** methanol, **c** and ethanol formation along with **d** selectivity map. Reaction conditions are at 593 K, 30 bar carbon monoxide, 60 bar hydrogen, 0.01 bar water, 0 bar methane/methanol/ethanol. The *colors* on the selectivity map are determined by weighting the *red*, *green*, and *blue* channels with the selectivity for ethanol, methanol, and methane respectively. *Points* represent binding to transition metal (211) surfaces; an *error bar* of 0.2 eV is shown to indicate the typical accuracy of calculated adsorption energies based on the RPBE functional [20]. Carbon and oxygen binding are formation energies of the adsorbed species are referenced to graphite and gas-phase O_2

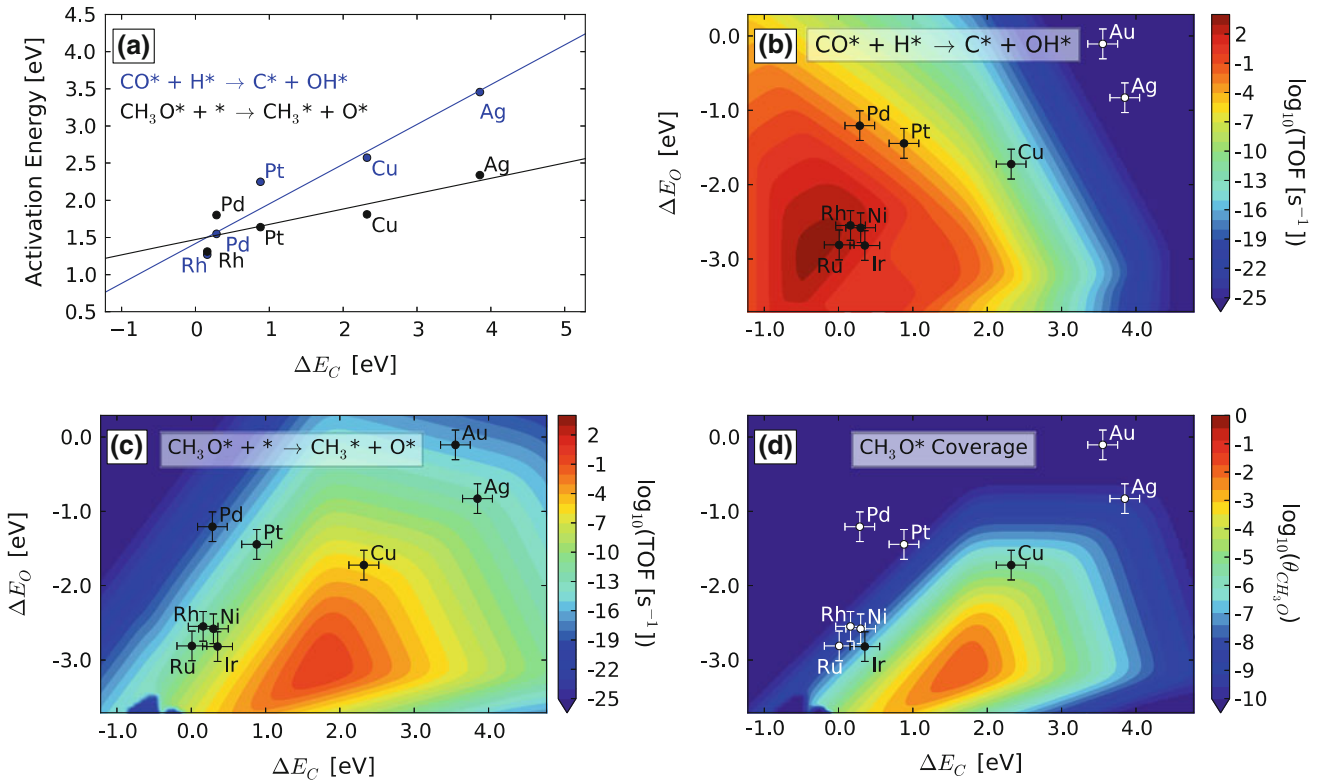

Fig. 2 **a** Activation energies for C–OH (*blue*) and O–CH_3 (*black*) bond splitting as a function of ΔE_C. **b** Calculated turnover frequencies (TOF) as a function of carbon and oxygen binding energies for hydrogen assisted CO dissociation and **c** CH_3O dissociation. **d** Coverage of methoxy intermediate as a function of ΔE_C and ΔE_O. Reaction conditions for (**b–d**) are the same as for Fig. 1

first maximum derives from the hydrogenation of CO to methane via splitting of the C–O bond in COH as described in earlier studies [21, 27]. The second maximum, which is considerably smaller, is obtained by consideration of methane formation via splitting of the C–O bond of the adsorbed methoxy intermediate (CH_3O). The CH_3O intermediate acts as a second carbon source here, making methane formation feasible for less reactive metals. This is due to the fact that C–O bond splitting in CH_3O has a lower barrier than the corresponding splitting of CO [23] as shown in Fig. 2a. For the more reactive metals C–O bond breaking occurs via hydrogen-assisted CO dissociation in a single reaction step as described in Ref. [27] (Fig. 2b). This work was able to reproduce both the low barrier and low prefactor that were found experimentally. That the C–O cleavage proceeds via CO rather than CH_3O can be attributed to the fact that the CH_3O coverage on the surface is very low while the CO coverage is close to 1 ML which offsets the lower barrier found for CH_3O. However, in the less reactive regions there is an appreciable formation rate of methoxy (Fig. 2d) as CO cannot be split easily and is hence hydrogenated first. The low barrier for methoxy dissociation leads to an appreciable rate of C–O bond scission in this region, as shown in Fig. 2c. Despite surmountable barriers, C–O bond cleavage via CHO and CH_2O occurs at much lower rates due to the low coverages of these intermediates under steady state conditions.

The methanol volcano shown in Fig. 1b is similar to earlier work [22]. The inclusion of multiple reaction sites on the surface (especially an extra site for hydrogen adsorption) does, however, shift this volcano towards slightly stronger oxygen binding energies. Cu is the only transition metal that is located close to the top of the volcano. It should be kept in mind that our analysis does not include hydrogenation of CO_2 which has been shown to be the main carbon source on Cu based catalysts for methanol synthesis [39, 40].

The ethanol volcano (Fig. 1c) consists of two distinct maxima similar to what is observed for methane formation. As discussed above for the methane volcano, these two maxima arise from the fact that there are two different pathways through which carbonaceous species can form on the surface. Carbon can be derived from the splitting of COH (leftmost volcano in Fig. 1a, c) or CO can be hydrogenated first to give CH_3O which is then split to yield CH_3 and O (rightmost volcano in Fig. 1a, c). Both methane and ethanol formation require CH_x intermediates. It is therefore not surprising that the maxima of both reactions are located at approximately the same carbon and oxygen binding energies. The top of methane formation via CO

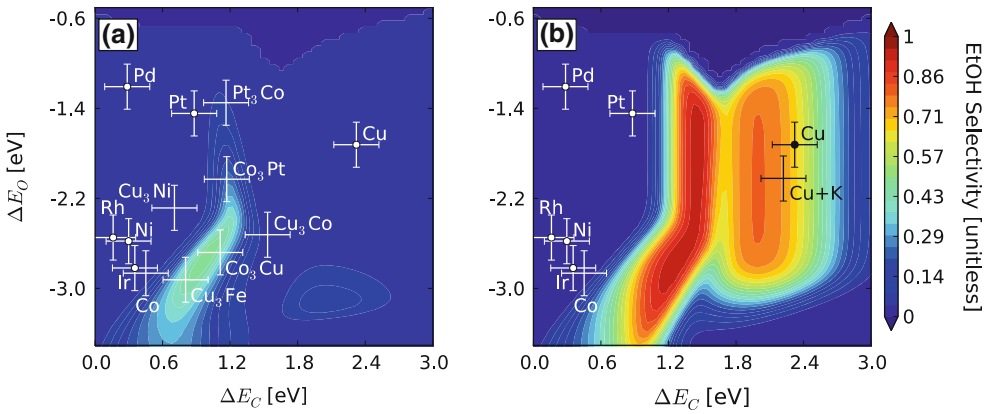

Fig. 3 Ethanol selectivity with methanol pressure of 0 bar (**a**) and 15 bar (**b**). All other reaction conditions and figure details are the same as for Fig. 1. *Points* marked with *circles* were used to construct scaling relations, while only carbon and oxygen binding energies were calculated for other points. Alloy binding energies correspond to the site which is most favorable for ethanol synthesis

splitting, however, is located at stronger carbon binding energies as compared to ethanol formation. Methanation rates are rather high and ethanol formation is rather slow leaving only a small window within which high selectivity for higher alcohols can be expected.

Figure 1d shows that none of the transition metals lies in the selectivity window for alcohols. The maximum selectivity towards ethanol occurs at $\Delta E_C = 0.95$ and $\Delta E_O = -2.65$, where the selectivity is 50 %, with the remainders being 25 % methane and 25 % methanol. We suggest that this is one reason it has proven difficult to find good higher alcohol synthesis catalysts. Our analysis also suggests several possible strategies for improving ethanol selectivity, explaining some of the catalyst promotion effects that have been found. Two main strategies are: (1) Either one can make Cu more reactive towards CO bond splitting or (2) make the early transition metals less reactive.

One well-tested method for tuning the reactivity of transition-metal catalysts is to modify the electronic structure of the metal by forming alloys or bi-component catalysts. Figure 3a shows a close-up of the ethanol-selective region of descriptor space, along with the carbon and oxygen binding energies of several interesting alloys. Many of these alloys are similar to previously discovered catalysts based on Cu and Co, or have been shown to be selective upon promotion with the depicted transition metals [8, 11, 41–43]. The alloys illustrate the "interpolation principle" [44] where the electronic structure sampled by the adsorbate in a mixed metal site becomes an intermediate between the properties of the individual metals [45]. It is likely that there are other alloys in the ethanol selectivity window, but a more detailed screening study is necessary to assess the stability, cost, and other relevant characteristics of these alloys. The electronic structure can also be modified by the use of alkali promoters. Figure 3b shows that the addition of potassium strengthens both carbon and oxygen binding of the Cu(211) surface moving Cu towards a region of higher oxygenate selectivity. In addition promotion with alkalis increases the rate of CH_x–O bond scission by lowering the barrier due to electrostatic effects as observed for e.g. N_2 splitting on Ru [46]. This effect will lead to increased higher alcohol production rates in the presence of alkali metals. Furthermore, the fact that CH_x–CO transition-states will likely have a significant dipole moment leads us to speculate that alkali metals may further increase oxygenate selectivity by lowering the CH_x–CO coupling barriers. In addition the presence of methanol during the higher alcohols synthesis reaction on Cu catalysts can further enhance selectivity and activity towards ethanol production as can be seen directly from Fig. 3b. We will discuss this effect in detail later on.

A different route to engineering the reactivity of transition-metal catalysts is by altering the geometric structure of the catalyst. Reducing the number of step/defect sites on catalysts in the methane region of descriptor space, or increasing the amount of low-coordination sites on the nobler metals could affect the alcohol selectivity. These geometric effects will be influenced by particle size, support interactions, promoters, etc. and are thus quite difficult to control in practice. The kinetic model we use considers only (211) sites, so we cannot make quantitative predictions about the role of defects; however, it is qualitatively clear that defects will decrease (increase) the alcohol selectivity for reactive (noble) metals. It is known that certain metal oxides block steps of transition metals [47] and it is possible that this is one of the effects of adding oxides to Fischer–Tropsch type catalysts to increase alcohol selectivity [9, 43]. We hypothesize that blocking of step and defect sites plays an important role in Rh catalysts that are selective towards higher alcohols. Figure 1d predicts that Rh(211) should be selective towards methane; however, it has been shown that the C–O bond breaking barrier is much higher on close-packed planes [27], which implies that methane synthesis rates will decrease on Rh(111) or other less reactive facets. Previous theoretical work has indicated that ethanol synthesis is feasible on Rh(111), especially in the presence of Mn dopants [16, 17]. The role of defects and control of site types is likely the reason that

small differences in catalyst preparation/support can have such significant influences on the alcohol selectivity on Rh and other catalysts [8]. Further studies are needed to understand the impact of multiple facets and site blocking on the activity and selectivity of higher alcohol catalysts in a more quantitative way.

The development of higher alcohol catalysts will require alloying/promotion of transition metals. These types of multi-component catalysts will inevitably consist of many different site types based on the distribution of the two components and the geometrical structure of the surface. It is important to note that, in reality, selectivity will be determined using the collective rate, which contains contributions from all site types. For this reason the existence of an active and selective site for alcohol synthesis is a necessary, but not sufficient, condition for a catalyst to be active and selective for higher alcohol synthesis. It is also necessary that the catalyst (or support) does not contain different active sites that produce methane/methanol at higher rates than the sites that produce ethanol. Therefore, the development of alcohol catalysts will depend not only on the discovery of new materials, but also on the optimization of the atomic-scale structure of these materials.

If catalysts that also make large amounts of methanol were employed in higher alcohol synthesis there would be an appreciable buildup of methanol in the reaction gas. We included this possibility by allowing the presence of methanol in our microkinetic model and investigated its effect on the selectivity to higher alcohols. Interestingly, methanol can act as a secondary carbon source and especially increases the CH_3O coverage. This leads to a higher rate of C–O bond scission due to the lower barrier of methoxy decomposition as indicated by Fig. 2. The presence of methanol may also further increase C–C coupling rates via direct methanol insertion [6], a reaction path not considered in our current model. The selectivity for ethanol in the presence of $\sim$10 % methanol is shown in Fig. 3b. The methanol partial pressure is greater than the equilibrium pressure of methanol at these conditions, thus excess methanol production is suppressed. The resulting selectivity shows a competition between methane/ethanol production, and it is clear that the region of ethanol selectivity has expanded substantially compared to Fig. 3a. In this case Cu becomes more selective towards ethanol, and this selectivity (and more importantly its activity) is increased substantially by promotion with potassium. The selectivity of other potential alcohol catalysts is also increased.

The fundamental difficulty in finding an active and selective higher alcohol catalyst is evident when comparing the activation barriers for C–H coupling, C–CO coupling, and C–OH dissociation. The competition between C–H and C–CO coupling determines the selectivity towards ethanol over methane, while the C–O bond breaking constitutes the rate-determining step for $\Delta E_C > \sim 0$. The activation barriers for these reactions are shown as a function of ΔE_C in Fig. 4. This figure indicates that C–OH dissociation will be rate limiting for all metals with $\Delta E_C > \sim 0$ eV, while the selectivity changes from methane to ethanol somewhere between Pt and Cu. The high C–O dissociation barrier for metals in the selective region leads to low rates of ethanol formation. Moreover, for less reactive metals methanol synthesis becomes competitive over C–O bond breaking changing the selectivity towards methanol.

Our theoretical study is conducted with a functional that does not account for van der Waals (vdW) forces, which are expected to play a role in longer chain species adsorbed on the surface [48]. It is therefore likely that the binding energies of intermediates involved in ethanol (or higher alcohol) formation are stabilized by these dispersion forces and that the rate of ethanol formation is actually higher than predicted here, increasing the window for ethanol formation to some extent. Furthermore, it should be kept in mind that the formation of Fischer–Tropsch products like alkanes and alkenes is not considered in our analysis. These molecules are usually produced on reactive transition metals like Co or Fe (or their oxides/carbides). Inclusion of the Fischer–Tropsch reaction will cut off the selectivity towards higher alcohols on the stronger binding end of

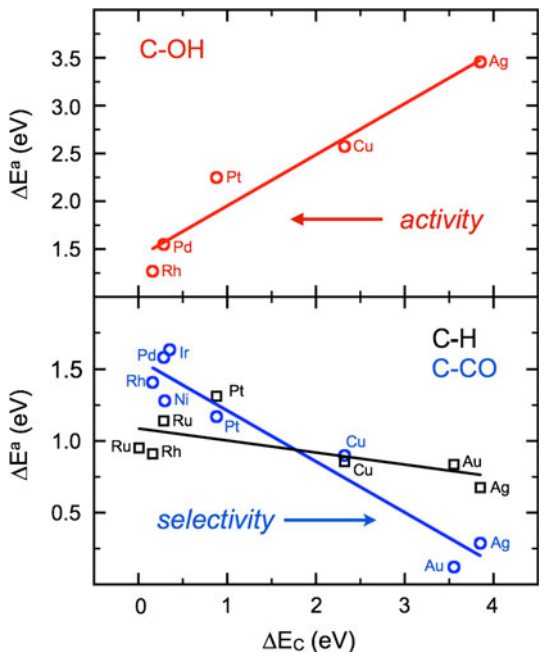

Fig. 4 Illustration of balance between ethanol activity and selectivity. Activation barriers for C–OH dissociation (*top panel red*), and C–CO (*bottom panel blue*) and C–H (*bottom panel black*) coupling are given as a function of ΔE_C for a number of 211 surfaces. Note that C–OH and C–CO/C–H have a different sign for the slope due to the fact that all barriers scale with the dissociated state. The activity increases as C–OH bond breaking gets easier while the selectivity towards ethanol increases when going in the opposite direction

oxygen/carbon binding energies, further reducing the selectivity window that has been identified for oxygenate production. Inclusion of alkanes as a potential product, vdW contributions and inclusion of other reaction mechanisms will be subject of future studies, but we expect that the conceptual picture presented here will remain the same.

4 Conclusions

We investigated one potential reaction path leading to higher alcohol formation with the use of scaling relations for adsorbates and transition states. These scaling relations allowed for the simplification of the complicated reaction network so that the reaction could be entirely described by two parameters. We further used microkinetic modeling of ethanol as well as methane and methanol formation, enabling the identification of a region where selective higher alcohol catalysts might be found. This region lies between the volcano for methanol and methane formation and there is only a small window where C–O bond cleavage is efficient enough to allow for the formation of surface carbon (that then react with CO to form CCO species) without methane formation being the dominant reaction. We note that our model of ethanol selectivity is numerically sensitive since division of reaction rates, which are exponentially dependent on activation energies, determines selectivity. The uncertainty associated with the scaling relations and electronic structure calculations is hence not properly accounted for in selectivity plots. In a more rigorous approach one could account for the uncertainty in order to obtain more quantitatively accurate estimates of selectivity; however, we expect that the general region where one can find selective catalysts will stay unchanged since trends are generally well-represented in DFT and descriptor-based analyses [31].

This work represents a first step towards understanding higher alcohol synthesis on transition-metal surfaces. Using a relatively simple kinetic model it is found that there are two distinct selectivity regions in descriptor-space (Fig. 1d): metals more reactive than Pt will be selective towards methane, while the nobler metals will favor methanol. This leaves only a small window where higher alcohol formation will be selective over methane and methanol (Fig. 4). Unfortunately no pure metal (211) surfaces lie in this region, which is likely the reason discovery of active and selective transition metal based higher alcohol catalysts has proven so difficult in practice. Despite this there are promising strategies to move catalysts towards the higher alcohol regime by modifying their electronic structure by alloying or the use of dopants to increase C–O bond scission (for methanol catalysts), block active sites for hydrocarbon production (for methanation catalysts) and increase CH_x–CO coupling rates. The findings suggest that an atomic-scale understanding of the system will be crucial for the discovery of new materials and requires the optimization of the active sites for selective higher alcohol production.

Acknowledgments Primary support by the U.S. Department of Energy (DOE), Office of Basic Energy Sciences to the SUNCAT Center for Interface Science and Catalysis is gratefully acknowledged (JKN, FS, FAP, ACL, AJM). In addition, AJM wishes to thank the Danish Ministry of Science, Technology and Innovation through the Catalysis for Sustainable Energy initiative, the Danish National Research Foundation and National Science Foundation through the Nordic Research Opportunity and Graduate Research Fellowship Program Grant No. DGE-1147470, and the Department of Defense (DoD) through the National Defense Science & Engineering Graduate Fellowship (NDSEG) Program.

References

1. Spath PL, Dayton DC (2003) Preliminary screening—technical and economic assessment of synthesis gas to fuels and chemicals with emphasis on the potential for biomass-derived syngas; NREL/TP-510-34929. Golden, National Renewable Energy Laboratory
2. Spivey JJ, Egbebi A (2007) Heterogeneous catalytic synthesis of ethanol from biomass-derived syngas. Chem Soc Rev 36:1514–1528
3. Subramani V, Gangwal SK (2008) A review of recent literature to search for an efficient catalytic process for the conversion of syngas to ethanol. Energy Fuels 22:814–839
4. Surisetty VR, Dalai AK, Kozinski J (2011) Alcohols as alternative fuels: an overview. Appl Catal A 404:1–11
5. Nunan JG, Bogdan CE, Klier K, Smith KJ, Young C-W, Herman RG (1989) Higher alcohol and oxygenate synthesis over cesium-doped Cu/ZnO catalysts. J Catal 116:195–221
6. Xu M, Iglesia E (1999) Carbon-carbon bond formation pathways in CO hydrogenation to higher alcohols. J Catal 188:125–131
7. Gupta M, Smith ML, Spivey JJ (2011) Heterogeneous catalytic conversion of dry syngas to ethanol and higher alcohols on Cu-based catalysts. ACS Catal 1:641–656
8. Matsuzaki T, Takeuchi K, Hanaoka TA, Arawaka H, Sugi Y (1993) Effect of transition metals on oxygenates formation from syngas over Co/SiO_2. Appl Catal A 105:159–184
9. Ichikawa M (1978) Catalytic synthesis of ethanol from CO and H_2 under atmospheric pressure over pyrolysed rhodium carbonyl clusters on TiO_2, ZrO_2, and La_2O_3. J Chem Soc, Chem Commun 566–567
10. Bhasin MM, Bartley WJ, Ellgen PC, Wilson TP (1978) Synthesis gas conversion over supported rhodium and rhodium-iron catalysts. J Catal 54:120–128
11. Courty P, Durand D, Freund E, Sugier A (1982) C1–C6 alcohols from synthesis gas on copper–cobalt catalysts. J Mol Catal 17:241–254
12. Subramanian N, Gao J, Mo X, Goodwin J, Torres W, Spivey JJ (2010) La and/or V oxide promoted Rh/SiO_2 catalysts: effect of temperature, H_2/CO ratio, space velocity, and pressure on ethanol selectivity from syngas. J Catal 262:204–209
13. Murchison CB, Conway MM, Stevens RR, Quarderer GJ (1988) Mixed alcohols from syngas over moly catalysts. In: Ternan M (ed) Proceedings of the 9th international congress of catalysis; Phillips. Chemical Institute of Canada, Ottawa, pp 626–633
14. Woo HC, Park KY, Kim YG, Nam IS, Chung JS, Lee JS (1991) Mixed alcohol synthesis from carbon monoxide and dihydrogen

over potassium promoted molybdenum carbide catalysts. Appl Catal 75:267–280
15. Christensen JM, Duchstein LDL, Wagner JB, Jensen PA, Temel B, Jensen AD (2012) Catalytic conversion of syngas into higher alcohols over carbide catalysts. Ind Eng Chem Res 51:4161–4172
16. Mei D, Rosseau R, Kathmann SM, Glezakou VA, Engelhard MH, Jiang W, Wang C, Gerber MA, White JF, Stevens DJ (2010) Ethanol synthesis from syngas over Rh-based/SiO_2 catalysts: a combined experimental and theoretical modeling study. J Catal 271:325–342
17. Choi Y, Liu P (2009) Mechanism of ethanol synthesis from syngas on Rh(111). J Am Chem Soc 131:13054–13061
18. Ferrin P, Simonetti D, Kandoi S, Kunkes E, Dumesic J, Nørskov J, Mavrikakis M (2009) Modeling ethanol decomposition on transition metals: a combined application of scaling and Brønsted–Evans–Polanyi relations. J Am Chem Soc 131:5809–5815
19. The Dacapo plane wave/pseudopotential code is available as opensource software at http://wiki.fysik.dtu.dk/dacapo
20. Hammer B, Hansen LB, Nørskov JK (1999) Improved adsorption energetics within density-functional theory using revised Perdew–Burke–Ernzerhof functionals. Phys Rev B 59:7413–7421
21. Lausche AC, Medford AJ, Khan TS, Xu Y, Bligaard T, Abild-Pedersen F, Nørskov JK, Studt F (2013) On the effect of coverage-dependent adsorbate–adsorbate interactions for CO methanation on transition metal surfaces. J Catal 307:275–282
22. Studt F, Abild-Pedersen F, Wu Q, Jensen AD, Temel B, Grunwaldt JD, Nørskov JK (2012) CO hydrogenation to methanol on Cu–Ni catalysts: theory and experiment. J Catal 293:51–60
23. Wang S, Temel B, Shen J, Jones G, Grabow LC, Studt F, Bligaard T, Abild-Pedersen F, Christensen CH, Nørskov JK (2011) Universal Brønsted–Evans–Polanyi relations for C–C, C–O, C–N, N–O, N–N, and O–O dissociation reactions. Catal Lett 141:370–373
24. Wang S, Petzold V, Tripkovic V, Kleis J, Howalt JG, Skúlason E, Fernández EM, Hvolbæk B, Jones G, Toftelund A, Falsig H, Björketun M, Studt F, Abild-Pedersen F, Rossmeisl J, Nørskov JK, Bligaard T (2011) Universal transition state scaling relations for (de)hydrogenation over transition metals. Phys Chem Chem Phys 13:20760–20765
25. Hummelshøj JS, Abild-Pedersen F, Studt F, Bligaard T, Nørskov JK (2012) CatApp: a web application for surface chemistry and heterogeneous catalysis. Angew Chem Int Ed 51:272–274
26. Monkhorst HJ, Pack JD (1976) Special points for Brillouin-zone integrations. Phys Rev B 13:5188–5192
27. Andersson MP, Abild-Pedersen F, Remediakis IN, Bligaard T, Jones G, Engbæk J, Lytken O, Horch S, Nielsen JH, Sehested J, Rostrup-Nielsen JR, Nørskov JK, Chorkendorff I (2008) Structure sensitivity of the methanation reaction: H_2-induced CO dissociation on nickel surfaces. J Catal 255:6–19
28. Grabow LC, Mavrikakis M (2011) Mechanism of methanol synthesis on Cu through CO_2 and CO hydrogenation. ACS Catal 1:365–384
29. Ojeda M, Li A, Nabar R, Nilekar AU, Mavrikakis M, Iglesia E (2010) Kinetically relevant steps and H2/D2 isotope effects in Fischer–Tropsch synthesis on Fe and Co catalysts. J Phys Chem 114:19761–19770
30. Ojeda M, Nabar R, Nilekar AU, Ishikawa A, Mavrikakis M, Iglesia E (2010) CO activation pathways and the mechanism of Fischer–Tropsch synthesis. J Catal 272:287–297
31. Nørskov JK, Abild-Pedersen F, Studt F, Bligaard T (2011) Density functional theory in surface science and catalysis. Proc Natl Acad Sci USA 108:937–943
32. Behrens M, Studt F, Kasatkin I, Kühl S, Hävecker M, Abild-Pedersen F, Zander S, Girgsdies F, Kurr P, Kniep BJ, Tovar M, Fischer RW, Nørskov JK, Schlögl R (2012) The active site of methanol synthesis over Cu/ZnO/Al_2O_3 industrial catalysts. Science 336:893–897
33. Bligaard T, Nørskov JK, Dahl S, Matthiesen J, Christensen CH, Sehested J (2004) The Brønsted–Evans–Polanyi relation and the volcano curve in heterogeneous catalysis. J Catal 224:206–217
34. Abild-Pedersen F, Greeley J, Studt F, Rossmeisl J, Munter TR, Moses PG, Skúlason E, Bligaard T, Nørskov JK (2007) Scaling properties of adsorption energies for hydrogen-containing molecules on transition-metal surfaces. Phys Rev Lett 99:016105
35. Jones G, Studt F, Abild-Pedersen F, Nørskov JK, Bligaard T (2011) Scaling relationships for adsorption energies of C2 hydrocarbons on transition metal surfaces. Chem Eng Sci 66:6318–6323
36. Pallassana V, Neurock M (2000) Electronic factors governing ethylene hydrogenation and dehydrogenation activity of pseudomorphic Pd_{ML}/Re(0001), Pd_{ML}/Ru(0001), Pd(111), and Pd_{ML}/Au(111) Surfaces. J Catal 191:301–317
37. Nørskov JK, Bligaard T, Logadottir A, Bahn S, Hansen LB, Bollinger M, Bengaard H, Hammer B, Sljivancanin Z, Mavrikakis M, Xu Y, Dahl S, Jacobsen CJH (2002) Universality in heterogeneous catalysis. J Catal 209:275–278
38. Michaelides A, Liu ZP, Zhang CJ, Alavi A, King DA, Hu P (2003) Identification of general linear relationships between activation energies and enthalpy changes for dissociation reactions at surfaces. J Am Chem Soc 125:3704–3705
39. Chinchen GC, Denny PJ, Parker DG, Spencer MS, Whan DA (1987) Mechanism of methanol synthesis from CO_2/CO/H_2 mixtures over copper/zinc oxide/alumina catalysts: use of ^{14}C-labelled reactants. Appl Catal 30:333–338
40. Sahibzada M, Metcalfe IS, Chadwick D (1998) Methanol synthesis from CO/CO_2/H_2 over Cu/ZnO/Al_2O_3 at differential and finite conversions. J Catal 174:111–118
41. Xu R, Yang C, Wei W, Li W, Sun Y, Hu T (2004) Fe-modified $CuMnZrO_2$ catalysts for higher alcohols synthesis from syngas. J Mol Catal A 221:51–58
42. Guczi L, Hoffer T, Zsoldos Z, Zyade S, Maire G, Garin F (1991) Structure and catalytic activity of alumina-supported Pt–Co bimetallic catalysts. chemisorption and catalytic reactions. J Phys Chem 95:802–808
43. Gnanamani MK, Ribeiro MC, Ma W, Shafer WD, Jacobs G, Graham UM, Davis BH (2011) Fischer–Tropsch synthesis: metal-support interfacial contact governs oxygenates selectivity over CeO_2 supported Pt–Co catalysts. Appl Catal A 393:17–23
44. Jacobsen CJH, Dahl S, Clausen BS, Bahn S, Logadottir A, Nørskov JK (2001) Catalyst design by interpolation in the periodic table: bimetallic ammonia synthesis catalysts. J Am Chem Soc 123:8404
45. Greeley J, Nørskov JK (2005) A general scheme for the estimation of oxygen binding energies on binary transition metal surface alloys. Surf Sci 592:104–111
46. Mortensen JJ, Hammer B, Nørskov JK (1998) Alkali promotion of N_2 dissociation over Ru(0001). Phys Rev Lett 80:4333–4336
47. Bengaard HS, Nørskov JK, Sehested JS, Clausen BS, Nielsen LP, Molenbroek A, Rostrup-Nielsen JR (2002) Steam reforming and graphite formation on Ni catalysts. J Catal 209:365
48. Tait SL, Dohnálek Z, Campbell CT, Kay BD (2006) *n*-Alkanes on Pt(111) and on C(0001)/Pt(111): chain length dependence of kinetic desorption parameters. J Chem Phys 125:234308